11

Nitroxyl Amide Spin Labeling: Methyl Esterification-, Hydration-, and Ca^{2+}-Induced Motional Perturbations of Pectinic Polysaccharides in Apples

Peter L. Irwin,* Walee Chamulitrat, Michael D. Sevilla,*** and Ann E. Hoffman***

**USDA, ARS, Eastern Regional Research Center, 600 E. Mermaid Lane, Philadelphia, PA 19118*
***NIH, Laboratory of Molecular Biophysics, P.O. Box 12233, MD 10-03, Research Triangle Park, NC 27709*
****Department of Chemistry, Oakland University, Rochester, MI 48063*

The cell walls of higher plants are structurally complicated, mostly polysaccharide, matrices that are economically important because they modulate cell structure, morphology and act as a barrier to small molecules (Darvill et al., 1980). Because of these characteristics, methods that proffer the ability to observe perturbations in the microscopic structure of the wall matrix, as a function of various treatments, could have an impact on the processing and storageability of plant products. The primary cell wall of most higher plants is a biphasic framework consisting of an infrastructure of cellulose microfibrils held together by a rigid gel-like lattice of matrix polysaccharides (Preston, 1979). These matrix polymers, which make up approximately two-thirds of the total primary cell wall and middle lamellar mass, are hydrophilic, polyhydroxy macromolecules that are extensively hydrated in vivo. Galacturonic acid-containing matrix polysaccharides in apples (Barrett and Northcote, 1965; Ben-Arie, Kisley, and Frenkel, 1979; Stevens

and Selvendran, 1984), frequently referred to as pectin or pectinic acid, are based on linear blocks, ca. 40–80 monomer units long (Irwin, Sevilla, and Chamulitrat, 1988), of α-(1→4)-linked *D*-galacturonic acid (homopolygalacturonans) interspersed with (1→2)- and (1→2 or 4)-substituted *L*-rhamnose. The *L*-rhamnoses are usually further linked with neutral polymers forming side chains. Further complicating the molecular picture is the fact that the C_6 carboxyl groups of the polyuronides are methyl esterified 50–70% (Irwin et al., 1985a) and possibly reside block-wise (Irwin, Sevilla, and Chamulitrat, 1988; Jarvis, 1984) in hydrophobic domains.

One of the more important functions of pectin in situ relates to its capacity to act as a cation exchange resin, thereby modulating mono- or divalent cation activity within the cell wall network. These acidic polysaccharides also manifest a cooperative-sequential binding mechanism (Irwin et al., 1984, 1985b) for divalent cations. The most characteristic physical property of the pectinic polysaccharides is their ability to form gels and aggregates under aqueous conditions (Cesaro et al., 1982; Fishman et al., 1984; Grant et al., 1973). The mutual interactions and attractions of various polysaccharides have been investigated in gels (Dea et al., 1977), and different types of intermolecular associations can be distinguished. Certain gel structures have been proposed to prevail through the exclusion of portions of the polymer chain and the realignment of stiff structures with more compatible geometries that result in mixed aggregates. The gel structure of polymer chains in cell wall matrices is much more difficult to ascertain because of the multifarious interaction of weak forces between adjacent chains. Thus, the higher-order structure of acidic polysaccharides in their natural, hydrated-solid state are not well understood because hydrogen bonding, hydration effects, and dipolar/ionic forces may interact in manifold ways to secure these macromolecules within the matrix in ordered arrays (Rees et al., 1982).

Electron paramagnetic resonance (EPR) spectroscopy is a premier technique to characterize the microscopic and dynamic features (Berliner, 1976) of numerous chemical species. Nitroxyl spin probes have been used widely to procure data about localized molecular attributes such as conformation, flexibility, and polymer–diluent interactions in diverse systems. Only within the last several years has a significant amount of research on spin-labeled carbohydrates been published (Gnewuch and Sosnovsky, 1986). Even less information is available about the utility of these methods for obtaining information on the microrheological properties of foods as discussed in this chapter. To this end, we have opted for the covalently bonded spin label method to study the rotational freedom between adjacent pectin molecules in apple cell walls (CW) or polygalacturonic acid (PGA) chains as they approach equilibrium hydration as a function of various levels of bound Ca^{2+} and/or degree of methyl esterification (Irwin, Sevilla, and Osman,

BASIC PRINCIPLES OF NITROXYL AMIDE SPIN LABELING

Excellent books (Swartz, Bolton, and Borg, 1972; Poole, 1983; Wertz and Bolton, 1986) have been devoted to the description of the basic EPR experiment and all its associated hardware; it is pointless to belabor what these fine texts do so well, and to these the reader is referred. Most spin labels are nitroxide free radicals that have the general structural formula

$$R_1 - C(CH_3)_2 - [NO] \dashv C(CH_3)_2 - R_2.$$

In this formula, R_1 and R_2 are side groups that give the nitroxide radical a certain degree of specialization for particular reactions with various functional groups (Wertz and Bolton, 1986). In our case, R_1 and R_2 are connected together to form a heterocyclic ring with a free amine, 4-amino-TEMPO or 4-amino-2,2,6,6-tetramethylpiperidine-1-oxyl (4*AT*), which we use to form an amide linkage with the C_6 carboxyl group (Fig. 11-1 insert; Irwin et al., 1991) of *D*-galacturonic acid in PGA or CW pectin. The methyl groups, which surround the N $\dashv$ O moiety, bestow a certain amount of protection of this functionality from being reduced rapidly to its hydroxyl amine (N–OH) form. Figure 11-1 shows a semilog plot of spin concentration of this same sample over a 3-year period when stored dry at room temperature; the bottom inset figure shows the calibration, necessary to perform periodically, to determine the best location within the microwave cavity for quantitation. These results reveal that our nitroxyl amide spin label, compared to other organic free radicals, is relatively stable over a long period of time ($\tau_{1/2} \sim 2$ years under less than ideal conditions). However, in the presence of a strong reducing agent, such as ascorbic acid (Fig. 11-2; Irwin et al., 1991), this same compound is reduced ($\Delta G^{300K} = -4.12$ kcal/mol) to its hydroxyl amine form within a few hours.

The type of EPR spectrum obtained for a nitroxide label depends on the chemical environment surrounding the label (e.g., hydrophobic, hydrophilic) as well as the rate ($1/\tau_R$ in units of s^{-1}) at which the nitroxide group can reorient or rotate about its magnetic x axis (Fig. 11-1 insert). If the nitroxide group is completely free to rapidly reorient about this axis (τ_R ca. 10^{-9} s or less) one observes a simple triplet (for our PGA nitroxyl amide label in solution $A_{isotropic} = \frac{1}{3}Tr\tilde{A} \sim 16$ G and $\tau_R \sim 0.9$–2.8 ns; Irwin, Sevilla, and Osman, 1987), due to the electron-nuclear hyperfine coupling with quadrupolar N ($I = 1$). As the environment surrounding a spin label changes, or

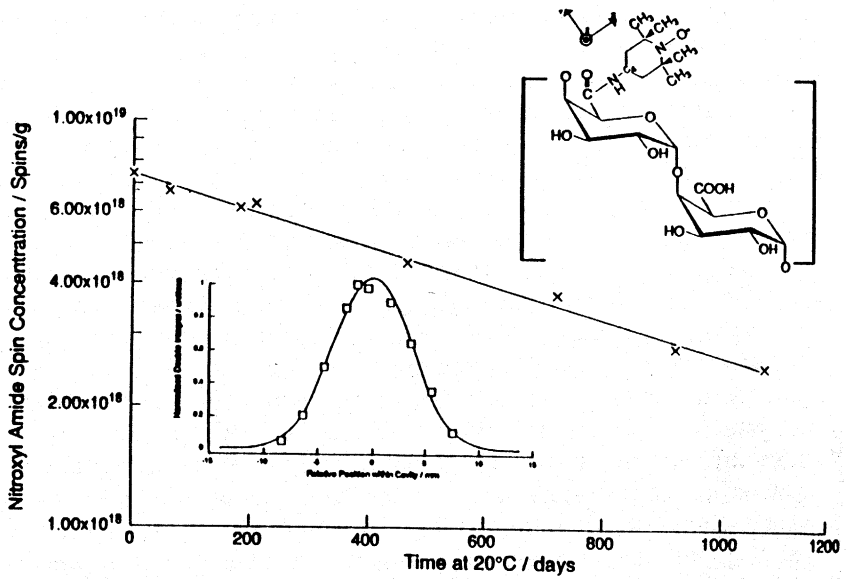

FIGURE 11-1. Semilog plot of PGA nitroxyl amide spin concentration as a function of time at ca. 293 K. Top inset figure: schematic of a nitroxyl amide spin-labeled galacturonan with the magnetic axes, x, y, and z, provided. Bottom inset: calibration of the ideal position of a sample within the cavity using a Cr^{3+}/Al_2O_3 crystal (11.38×10^{15} spins). Various spectral parameters (A_{zz}, $A_{isotropic}$), in units of Gauss, were calibrated against the 87.3 G hyperfine splitting of dilute Mn^{2+} in an MgO matrix. The parameters, g_{iso} or g_{zz}, were calibrated against Cr^{3+} in an MgO matrix ($g_{isotropic} = 1.9796$). The number of nitroxyl spins was calculated against the Cr^{3+}/Al_2O_3 crystal.

becomes more rotationally restrictive, the lineshape of the spectrum changes, because molecular motion does not sufficiently average anisotropies in the local environment, resulting in broadened linewidths and nonzero off-diagonal matrix elements for $\tilde{g}$ and $\tilde{A}$ (tensors of the 0th [scalar], 1st [vector] and 2nd ranks are herein represented as n, n or ñ, respectively).

The Covalent Attachment of the Spin Label, 4AT, to Acid Sugars

The general reaction (Hoare and Koshland, 1967; Taylor and Conrad, 1972) of water soluble carbodiimides with polyuronides and subsequent nucleophilic attack by 4AT is shown in Figure 11-3. In all the labeling performed herein (Irwin, Sevilla, and Osman, 1987; Chamulitrat et al., 1988; Chamulitrat and Irwin, 1989; Irwin et al., 1991) the carbodiimide utilized was 1-ethyl-3-(3-dimethylaminopropyl)carbodiimide (EDC). Previously, Hoare and Koshland (1967) have shown that reaction 1 (Fig. 11-3) proceeds rapidly

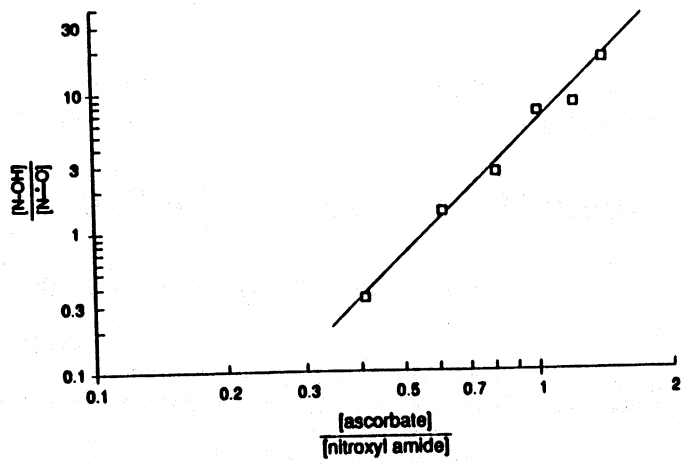

FIGURE 11-2. Log–log plot of $\frac{[N-OH]}{[N-O]}$ as a function of the molar ratio of ascorbate and bound N – O before reduction. Prior to reduction, the PGA amide sample had ca. 10% of the carboxyl groups, upon activation with EDC, reacted as the amide.

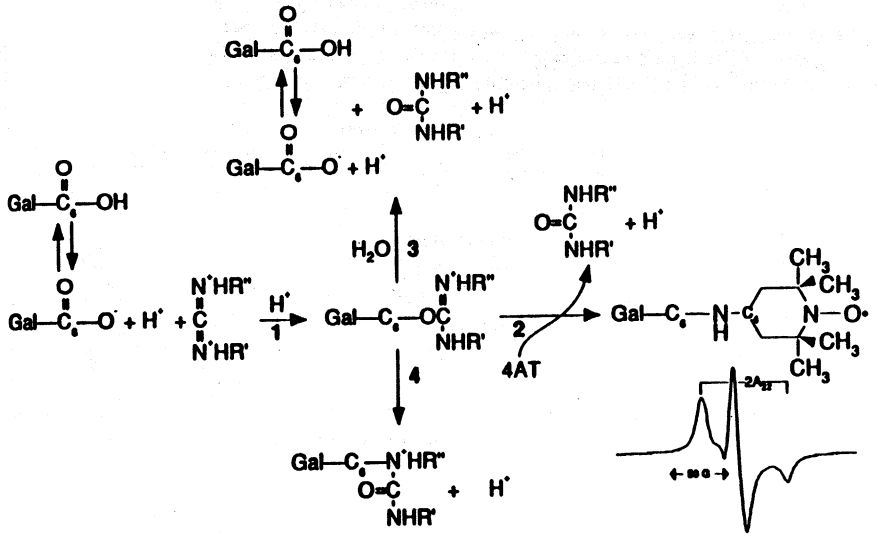

FIGURE 11-3. Reactions of uronic acids with carbodiimides (see also: Hoare and Koshland, 1967; Taylor and Conrad, 1972).

with the uptake of ca. 1 mol of H^+ per mol of acid depending on the ionization constant $\left(\frac{[A^-]}{[AH]}\right)$ and the reaction pH (Taylor and Conrad, 1972) (Fig. 11-4); this latter notion is readily supported by the fact that the predicted ionization constants (Daniels and Alberty, 1975) were close to those derived experimentally. In the presence of a high concentration of a strong nucleophile, such as 4*AT*, reaction 2 proceeds with the formation of our nitroxyl amide. High-resolution ^{13}C NMR (Irwin, Sevilla, and Osman, 1987) spectroscopic data of the reaction products show no evidence of N-acylurea (Fig. 11-3, reaction 4).

The Spatial Organization of Nitroxyl Amides in Acid Sugar Polymers

Interestingly (Irwin, Sevilla, and Osman, 1987), upon reaction and subsequent dialysis, we observed a significant degree of line broadening in partially reacted PGA powders (Figs. 11-5 and 11-6) arguing that the 4*AT*s were selectively reacting with carbodiimide-activated carboxyl groups in relatively small blocks or linear arrays rather than randomly throughout the polyanionic matrix. Generally speaking, when a system of electron spins, **s**, interacts with an applied magnetic field, **H** ($\mathbf{H}_{applied} + \mathbf{H}_{local}$), to produce a resonance line, each magnetic moment precesses about the **z** component of **H** with a frequency proportional to H_z. The scalar value as well as orientation of **H** will vary from one label to the next if there is a high-spin density, which results in a significant $H_{z,local}$ field contribution, and causes a smearing out of the observed precessional frequencies, thereby resulting in line broadening (Pryce and Stevens, 1950). Such dipolar broadening is theoretically described by the Hamiltonian (H) operator,

$$H_{dipolar} = g^2\beta^2 \sum_{i>j} \left\{ \frac{\mathbf{s}_i \cdot \mathbf{s}_j}{\mathbf{r}_{ij}^3} - 3\frac{[\mathbf{r}_{ij} \cdot \mathbf{s}_i][\mathbf{r}_{ij} \cdot \mathbf{s}_j]}{\mathbf{r}_{ij}^5} \right\}$$

In this relationship g, β, and **s** have their usual meaning (Abragam and Bleaney, 1970; Leigh, 1970; McMillan, 1968; Van Vleck, 1948) and **r** is the distance vector between the ith and jth spins. The summation subscript, $i > j$, identifies that each pair of dipolar interactions should be counted only once. Exact computation of $H_{dipolar}$ is not feasible but can be statistically evaluated by the method of moments first developed by Van Vleck (1948). The second moment ($\langle H^2 \rangle_{ave}$), which is related to a Gaussian's first deriva-

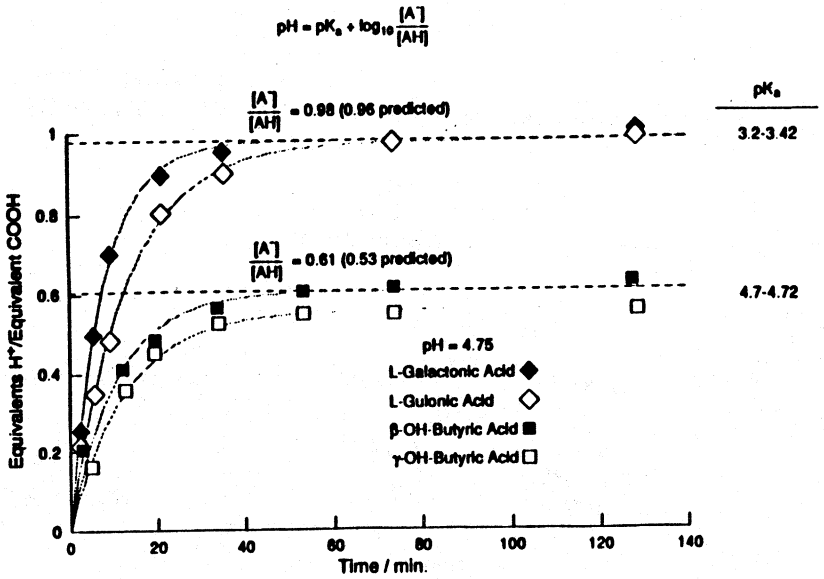

FIGURE 11-4. Acid uptake in the carbodiimide reaction (used with permission: Taylor and Conrad, 1972) with various hydroxy acids at pH 4.75. Reaction conditions: 0.2 mmol of each carboxylic acid and 0.2 mmol of the carbodiimide, 1-cyclohexyl-3-(2-morpholinoethyl)carbodiimide metho-*p*-tolulenesulfonate (CMC), in 20 ml of H_2O. As with our *4AT* reactions, the pH was maintained at 4.75 by automatic titration with 0.1 M HCL. For this chapter, the original data have been fit to the exponential,

$$\frac{[H^+]_{added}}{[COOH]} = \lim_{t\to\infty} \frac{[H^+]_{added}}{[COOH]} [1 - \exp(-tk)],$$

and iteratively solved for both the t_∞ limit as well as the rate constant, k, whereupon

$$\left\{\frac{[A^-]}{[AH]}\right\}_{obs.} = \lim_{t\to\infty} \frac{[H^+]_{added}}{[COOH]}.$$

In these calculations, we found that $k = 7.64\ h^{-1}$ and $4.65\ h^{-1}$ for L-galactonic and L-gulonic acids, respectively; we also established that $k = 5.6\ h^{-1}$ and $4.7\ h^{-1}$ for β-OH-butyric and γ-OH-butyric acids.

tive linewidth ($\Delta H_{pp} = 2\langle H^2\rangle_{ave}^{1/2}$), is defined as

$$\langle <H^2\rangle_{ave} = \int_{-\infty}^{\infty} (H - H_o)^2 f(H) dH \Big/ \int_{-\infty}^{\infty} f(H) dH.$$

Figure 11-5 shows digitally calculated $\langle H^2\rangle_{ave}$s for typically broadened 1st derivative nitroxyl amide PGA (Fig. 11-5, insert spectrum) powders, and

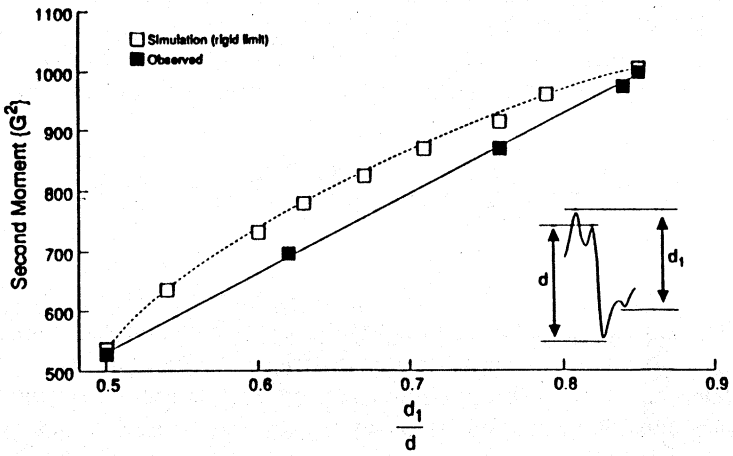

FIGURE 11-5. Relationship between the second moment ($\langle H^2\rangle_{ave}$), derived from numerical integrations, and the linewidth parameter $\frac{d_1}{d}$ (defined in the inset figure), whereupon $\langle H^2\rangle_{ave}$ was calculated digitally as

$$\langle H^2\rangle_{ave} = \frac{\Delta H}{\Delta H^2 \sum_{j=1}^{m}\sum_{i=1}^{I}\left\{\frac{\delta I(H)}{\delta H}\right\}_i} \sum_{j=1}^{m}\sum_{i=1}^{I} (H_j - H_o)^2 \left\{\frac{\delta I(H)}{\delta H}\right\}_i.$$

In the previous empirical relationship, $(\delta I(H)/\delta H)_i$ represents the relative amplitude of each first derivative data point, ΔH the field separation between points, and H_o the magnetic field scalar value where the double integral was half maximum (e.g., the center of the spectrum) (from Irwin et al., 1987, with permission).

corresponding rigid limit simulations as a function of an empirical broadening parameter, $\frac{d_1}{d}$. If one considers calculations for a randomly oriented lattice (Van Vleck, 1948; Irwin, Sevilla, and Shieh, 1984; Irwin, Sevilla, and Stoudt, 1985b) the following relationships are valid:

$$\langle H^2\rangle_{ave} = \frac{3}{5} g^4\beta^4 h^{-2} S(S+1) \sum_{i>j} \frac{1}{r_{ij}^6}$$

and

$$\sum_{i>j} \frac{1}{r_{ij}^6} = \left\{\frac{\kappa^2}{d^6}\right\}$$

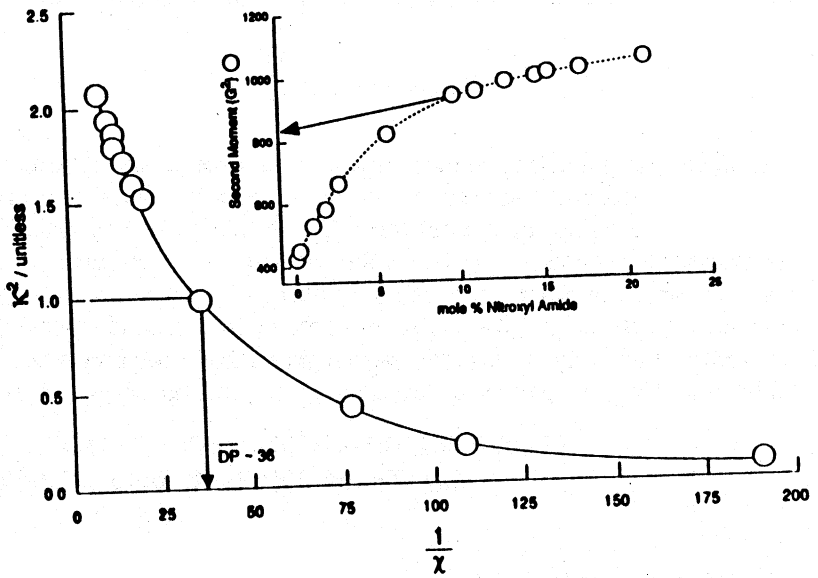

FIGURE 11-6. Plot of κ^2 for a PGA-bonded 4*AT* lattice versus reciprocal χ (from Irwin et al., 1988, with permission). Inset figure: Dependency of the nitroxyl amide's $\langle H^2 \rangle_{ave}$ on the molar ratio of spin-dimers to the total anionic ligand monomers (χ).

Thus, assuming that only dipolar spin–spin interactions occur, $\langle H^2 \rangle_{ave}$ is related to the reciprocal 6th power of the distance between a group of i–jth interacting spins. In the previous equations, d is the nearest neighbor distance parameter for an ordered array, and κ varies with the lattice disposition. We have utilized the κ term because changes in $\langle H^2 \rangle_{ave}$ cannot be attributed entirely to the nearest neighbor distance parameter. As a paramagnetic species begins to fill the lattice, an increase in the number of dipolar spin–spin interactions will occur at each ith spin. For example, $\kappa = 1$ for two interacting spins, 1.4 for a linear array, 2.45 for a two-dimensional (2-D) hexagonal array with six nearest neighbors, and $\kappa = 3.46$ for a three-dimensional (3-D) hexagonal close packing array with 12 nearest neighbors. Thus, considering nearest neighbor interactions only, κ^2 is an estimate of the number of dipolar interactions at distance d even in a system with an extended array caused by the decreased weighting of distant interactions. As κ approaches 1, we have found that κ^2 provides an accurate estimation of the number of near neighbor interactions per nitroxyl amide (Fig. 11-6; Irwin, Sevilla, and Chamulitrat, 1988), because, in this low concentration region, the number of distant interactions would be negligible. We can approximate

the dimer-only nearest neighbor distance parameter from the extrapolated zero concentration-$\langle H^2 \rangle_{ave}$ intercept (Fig. 11-6, at arrow); at this value of $\langle H^2 \rangle_{ave}$, κ is about 1. Assuming that d remains relatively constant with addition of the paramagnetic species, we can calculate the number of strongly interacting spins per ith point dipole using the previous expressions from each of the empirically derived values of $\langle H^2 \rangle_{ave}$. The concentration of bound paramagnetic species at which the number of dipolar spin–spin interactions is approximately 1 is related to the size of the homopolygalacturonan blocks, because the probability of bonding at near neighbor sites is far more likely than any other position within that same block. Because of this type of amide bonding, we can assume, as a first approximation, that one spin label pair bonds per polymer block within the matrix when κ is approximately 1. If this assumption is true the polymer's average degree of polymerization ($\overline{DP}$) can be estimated from χ when $\kappa = 1$,

$$(1/\chi)_{\kappa \sim 1} = \overline{DP},$$

whereupon χ is the mole fraction of paramagnetic dimers bound. For PGA the $\overline{DP}$ was found (Irwin, Sevilla, and Chamulitrat, 1988) to be ca. 36 and approximately agrees with the $\overline{DP}$ obtained from reducing end-group titration (Fishman et al., 1984) for these same compounds. The electron spin-lattice relaxation time (T_1) is related to interspin distances (Eaton and Eaton, 1978; Hyde and Rao, 1978). If the nitroxyl amide line broadening discussed earlier was due to relatively short interspin distances, as we maintain, the disruption of the PGA nitroxyl amide lattice, through ascorbate reduction (Fig. 11-2) or by competitive reactions with a nonparamagnetic amine of similar size (e.g., aniline), should induce a corresponding increase in a parameter, $\sqrt{T_1 T_2} \div T_{2,est}$ ($= T_{1\bullet}$; $1/T_{2,est} = \{\gamma\sqrt{3}\Delta H_{pp}\}/2$), related to T_1; $T_{1\bullet}$ is calculated from changes in the relative intensity of the centermost 1st derivative N ∴ O component of the low-power portion of a power saturation experiment, as described by Poole (1983, p. 593; see Fig. 11-11 for a typical saturation experiment). The data in Figure 11-7 clearly illustrate this principle. Upon reducing part of the nitroxyl's spin or reacting PGA with both 4*AT* and aniline, in the presence of EDC, the effect on relative $T_{1\bullet}$ was substantial. The nitroxyl amide $T_{1\bullet}$*s* increased by a factor of about 4 upon reduction with ascorbate to a total spin concentration of approximately 0.6 mol % N ∴ O ([N ∴ O]/[N − OH + N ∴ O] = 0.055). The relaxation time parameter was even more influenced in the aniline-reacted polymer than by partial reduction; this observation is ostensibly due to the fact that aniline has a smaller pK_a than 4*AT*, and, therefore, more amines are available to react (e.g., unprotonated) at this pH (4.75); therefore, more anilide functional groups are covalently bound than reduced 4*AT*-amides and result

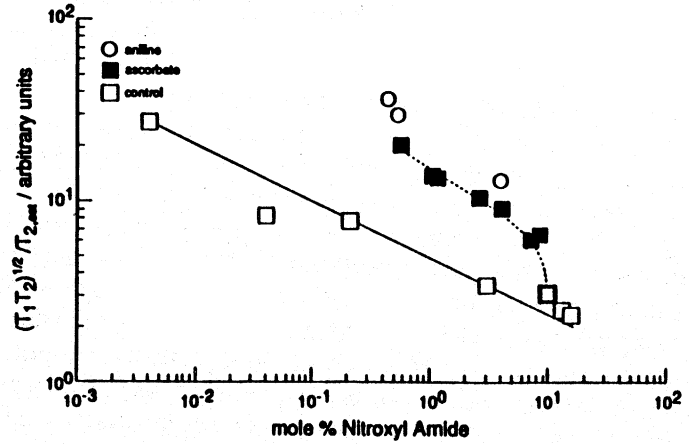

FIGURE 11-7. Relationship between covalently bound $4AT$ and the electron spin-lattice relaxation time-related parameter relative to that predicted for the untreated matrix (control), ascorbate reduced (partial), and aniline reacted. All ascorbate treatments were performed on the sample represented by the boldly highlighted open square (from Irwin et al., 1987, with permission).

in greater nitroxyl amide spacing. It is also likely that the reduction of the nitroxyl amide polymer is not completely random because the slope of the line, shown in Figure 11-2, is less than unity (e.g., negatively cooperative; Irwin et al., 1991).

RESOLVING PGA AND CW NITROXYL AMIDE "LOCAL" AND "INTERNAL" MOTIONS

Dehydrated PGA's nitroxyl amide spectra, measured at 77 K, were simulated using a rigid limit program (Chamulitrat et al., 1988) to obtain accurate $\tilde{g}$ and $\tilde{A}$ tensor components. These simulations applied Simpson's numerical integration over θ and ϕ, which are the angles between H and z themselves as well as their projection in the rotating frame. The spectral parameters, A_{zz} and g_{zz}, were measured empirically from the separation between the outer hyperfine extrema ($2A_{zz}$) and the midpoint of the two extrema, respectively. The orientationally dependent linewidth used to fit spectra had the form of

$$\frac{1}{T_2} = \alpha + \beta\cos^2\theta.$$

A Lorentzian lineshape provided the best simulations of the experimental EPR spectra. Parameters which gave the best fit were: $A_{xx} = 7.0$ G, $A_{yy} =$

4.5 G, $A_{zz} = 35.8$ G; $g_{xx} = 2.0095$, $g_{yy} = 2.0059$, $g_{zz} = 2.0022$; the orientation-dependent linewidth parameters, α and β, were found to be 5.8 G and 0.2.

Detailed simulations (Chamulitrat et al., 1988), using Stochastic Liouville theory (Freed, 1976), indicated that the preferred axis of rotation, x, was about the magnetic y-axis of the nitroxyl amide (Fig. 11-1, insert). These simulations were performed assuming that the rotational diffusion tensor, $\tilde{R}$, was axially symmetric about x. The best simulations of this type show that the nitroxyl amide moiety's preferred motion in the molecular frame was approximately about PGA's main axis. The best model for reorientation was the moderate jump. At low temperatures, spectral lineshape was mainly sensitive to local motions predominantly about the NH–C_4 bond because the CO–NH bond had an appreciable double-bond character. An energy of activation (E_a) of 0.39 kcal/mol (Fig. 11-8, open circles; $\log_e(1/\tau_R) = \log_e(1/\tau_{R,o}) - E_a/RT$) was estimated for the temperature range 141–271 K from the detailed simulation-derived $\tau_R s$. For comparison purposes, empirical $\tau_R s$ (Fig. 11-8, open squares) were also calculated as

$$\tau_R = a\left\{1 - \frac{A_{zz'l}}{A_{zz'rl}}\right\}^b$$

whereupon $A_{zz'l}$ is A_{zz} observed at a given temperature, and $A_{zz'rl}$ is that of the rigid limit; the parameters a and b are supplied in Table 11-1 for different models of diffusion and linewidths. Henceforth, for simplicity's sake, the low temperature range $\tau_R s$, where E_a is small, will be alluded to as $\tau_R s$ caused by "local" motions, while those in the higher temperature range will be referred to as "internal" motions, because the latter type are predominantly due to reorientation about the axis, which closely corresponds to PGA's main

TABLE 11-1 Parameters and Calculated Activation Energies (SE = ±0.05 kcal/mol) for Different Models of Rotation

Diffusion Model	Line-width/G	a	b	E_a/kcal/mol 179–233 K	E_a/kcal/mol 233–342 K
Brownian Diffusion	0.3	2.57×10^{-10}	−1.78	0.83	3.91
	3.0	3.40×10^{-9}	−1.36	0.63	5.14
Moderate Jump	0.3	6.99×10^{-10}	−1.20	0.55	3.00
	3.0	1.10×10^{-9}	−1.01	0.47	3.46
Strong Jump	0.3	2.46×10^{-10}	−0.59	0.27	1.69
	3.0	3.40×10^{-9}	−0.62	0.28	1.77

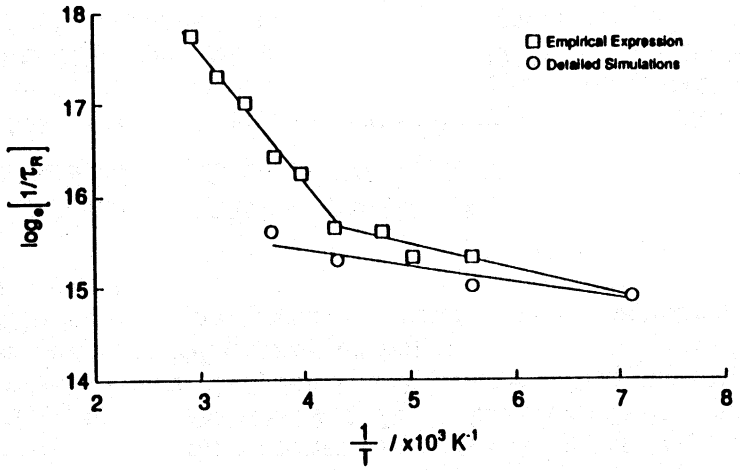

FIGURE 11-8. Arrhenius plots of reorientational motion of nitroxyl amide spin-labeled PGA using detailed simulations and an empirical expression (from Chamulitrat et al., 1988, with permission).

chain. Structural evidence that the higher temperature range $\tau_R s$ was due to the nitroxyl amide's reorientation along the homopolygalacturonan main chain is presented in Figure 11-9 (Chamulitrat and Irwin, 1989), where there was observed to be an increase in E_a as a function of Ca^{+2}_{bound} in both PGA and native apple cell wall matrices. These data indicate that Ca^{+2} cross-links more efficiently in PGA than in the CW matrix probably because the native polyanionic lattice is disrupted by methyl esterified uronosyl monomers as well as relatively large side chains. Enzymatic deesterification (Table 11-2) of the apple CW caused the internal motion $E_a s$ to approach those of PGA and argues that the nitroxyl spin labels are providing spatially specific information on $Ca^{+2}s$ effects at or near cell wall methyl ester domains. When our nitroxyl amine is specifically reacted (Chamulitrat and Irwin, 1989; Irwin, Sevilla, and Chamulitrat, 1988) with the cell wall matrix acid sugar polymers (Fig. 11-10, upper-most spectrum) to form the nitroxyl amide the cross-polarization and magic angle sample spinning NMR (CP-MAS/NMR) methyl ester resonance disappears; this apparent broadening effect is completely reversible by reduction of the nitroxyl (N – O) to the hydroxyl amine (N–OH) with ascorbate (Fig. 11-2, bottom spectrum). The illusory diminution of this methyl ester resonance could be due to several mechanisms (Eaton and Phillips, 1965; Gerasimowicz, Hicks, and Pfeffer, 1984; Redfield, 1965): the paramagnetic amide's effect on (1) rotating-frame spin-lattice relaxation, (2) the spectral density of this resonance, or (3) "T_1-

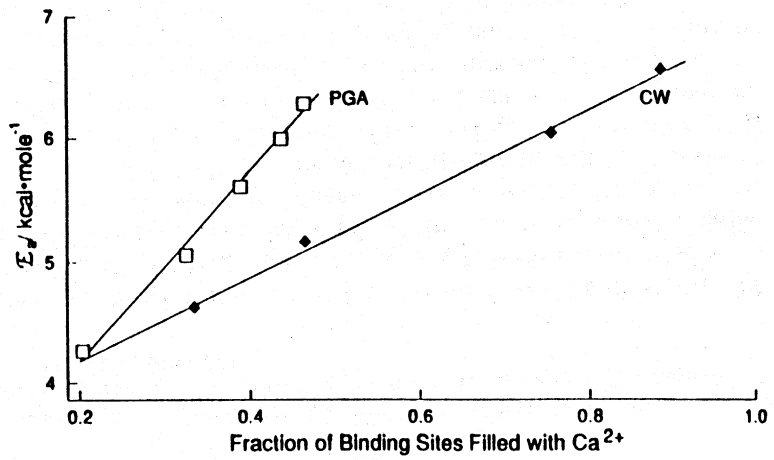

FIGURE 11-9. Internal motion $E_a s$ as a function of the fraction of binding sites occupied by Ca^{2+} for 4-*AT* spin-labeled PGA and apple CWs (from Chamulitrat and Irwin, 1989, with permission).

driven T_{2e}" whereupon that part of the free induction decay (FID) associated with the *O*-methyl resonance was not sampled because of a rapid loss of the FID envelope in the "dead time" prior to data acquisition. Regardless of the mechanism, these data support the hypothesis that the nitroxyl amides react close to the methyl ester hydrophobic domains. Interestingly, CW nitroxyl amide's relaxation properties were not much modulated by Ca^{+2} cross-links (Fig. 11-11; Irwin et al., 1991) because our relaxation parameter, $\sqrt{T_1 T_2}$, as measured by power saturation, were similar in Ca^{+2}-treated and control matrices. However, for inhomogeneously (anisotropic interactions in randomly oriented systems in the solid state) broadened samples such as these, Metz, Völkel, and Windsch (1990) have recently demonstrated that perhaps a better measure of spin-lattice relaxation ($\sqrt{T_1 T_{2e}}$) can be obtained from the microwave power where maximal signal intensity P_μ^{max}) is observed, assuming: (1) a Lorentzian lineshape, (2) H_1 (the microwave field scalar value in units of G) = $\sqrt{P_\mu}$ (in units of watts) (Poole, 1983)

$$\{T_1 T_{2e}\}^{1/2} \propto \{1/P_\mu^{max}\}^{1/2},$$

and (3) T_{2e} (a measure of H inhomogeneity) remains the same for simila samples, such as ours, and is much less than T_2. For the Ca^{+2}-treated PG (Fig. 11-11 insert: squares) sample the P_μ^{max} was ca. 22.18 mW, while that o the control (Fig. 11-11 insert: diamonds) was ca. 34.68 mW indicating tha the relative $\sqrt{T_1 T_{2e}}\, s$, as defined earlier, were approximately 20% larger afte

TABLE 11-2 Calculated Activation Energies for Nitroxyl Amide Internal Motion Between 233 and 358 K

	E_a/kcal/mol	
Sample	Moderate Jump	Brownian Diffusion
PGA	3.37	4.99
Control CW	2.46	3.66
PME	3.57	5.30

E_as were calculated from the empirical formula, $\tau_R = a\left\{1 - \frac{A_{ss'l}}{A_{ss'rl}}\right\}^b$, where $a = 6.99 \times 10^{-10}$ or 2.57×10^{-10} and $b = -1.2$ or -1.78 for moderate jump or Brownian diffusion models, respectively.

the Ca^{2+} treatment. Accurate P_μ^{max}s were obtained from the value of $\sqrt{P_\mu}$ where the 1st derivative empirical biexponential curve fit $((\delta I(H)/\delta H)_{max}$-vs-$\sqrt{P_\mu})$ with respect to $\sqrt{P_\mu}$ approached 0. Relaxation parameters can also be calculated (Fig. 11-12; Irwin et al., 1991) from the nonlinear numerical method of Metz, Völkel, and Windsch (1990); this method is problematic, especially with relation to the spin–spin relaxation time, T_2, as exemplified (Fig. 11-12, inset) by the fact that T_1 and T_2 are positively linear,

$$\text{slope} = T_{2\bullet}^2 \left\{\frac{\delta T_1}{\delta T_2}\right\} = +0.34 \text{ (assuming } T_{2\bullet} \text{ constant)},$$

with respect to each other. Of course, one would expect that as the uronosyl nitroxyl amide τ_Rs for internal motions increase (e.g., $\tau_{R,CW} > \tau_{R,CaPGA} > \tau_{R,PGA}$) to the point where $T_1 > T_2$, T_2 should subside (Bloembergen, Purcell, and Pound, 1945) and T_1 and τ_R increase. Regardless, this new technique does provide a reasonable way to measure $\sqrt{T_1 T_2}$ s without assuming H_1 is equivalent to $\sqrt{P_\mu}$, which was required by the linear technique displayed in Figure 11-11.

EQUILIBRIUM HYDRATION-INDUCED CHANGES IN MAIN CHAIN MOTION

Under ordinary circumstances, the primary wall and middle lamellar network of apple cortical cells are moderately (30–50% [wt/wt]) to fully hydrated (> 50% [wt/wt]; Chamulitrat et al., 1988). The higher order structure of cell wall matrix homopolygalacturonans are modulated to a significant

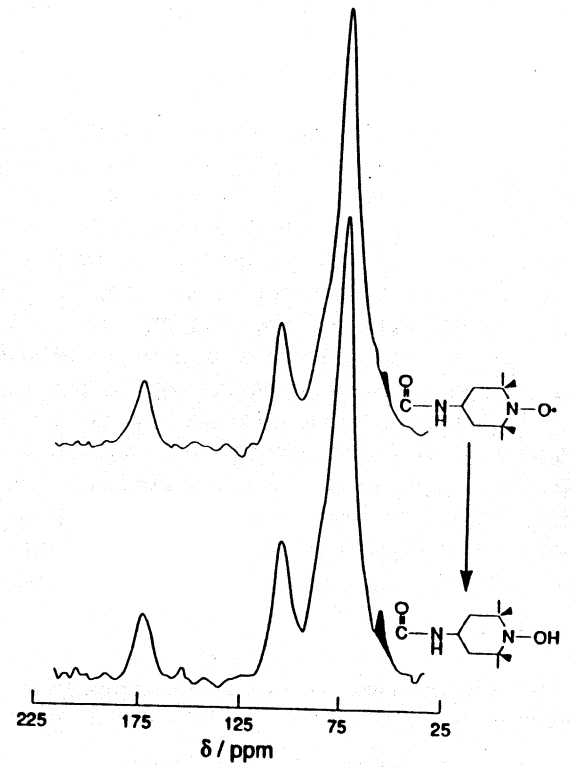

FIGURE 11-10. CPMAS/NMR spectra of apple CW matrices (0.8 ms of ^1H-^{13}C thermal contact) as a function of N ⇌ O (top spectrum) or as its reduced, N-OH, form (from Irwin et al., 1988, with permission).

degree by bound water molecules (Irwin, Sevilla, and Stoudt, 1985b). Knowledge about the spatial deformations, as measured by relative molecular flexibilities at different levels of hydration, may assist in the clarification of the higher order structure of sugar acid containing matrix polysaccharides.

Both CW and PGA nitroxyl amides hydrate over time at 100% relative humidity in a remarkably similar fashion (Fig. 11-13; Irwin et al., 1991) considering their extreme disparity in molecular constituency (e.g., only ca. 25% of the CW is made up of uronosyl residues and a large portion of these are methyl esterified; Irwin et al., 1985a), albeit the equilibrium level of hydration for PGA was ca. 25% greater. In order to analyze the hydration process from the standpoint of the nitroxyl amide moiety (Fig. 11-14), we have determined both the number and electron-nuclear distance (r) of nitroxyl amide bound ^2H_2O in hydrated spin labeled PGA. These data were obtained at 4.2 K using a three-pulse electron spin-echo modulation (ESE)

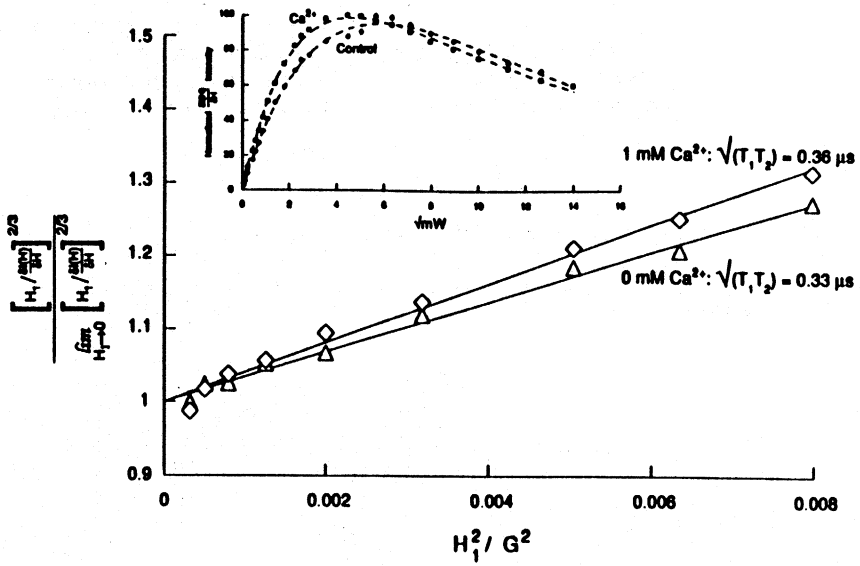

FIGURE 11-11. Power saturation plot of transformed $\frac{\delta I(H)}{\delta H}$ as a function of the square of the microwave perpendicular field, H_1^2 (in units of G^2). The original data, $\frac{\delta I(H)}{\delta H}$, are the first derivative intensity of the center ($m = 0$) N – O peak. We have made the assumption that $H_1 \propto \sqrt{P_\mu}$ (the microwave power output in units of Watts and Poole, 1983) and the constant of proportionality does not change from sample to sample (freeze-dried solids). Inset figure: complete power saturation curve and empirical curve fit for both Ca^{2+} and control PGA $4AT$ nitroxyl amides as a function of $\sqrt{P_\mu}$ (in units of $mW^{1/2}$). The empirical curve fit equation used was of the simple biexponential form,

$$I' = \frac{I'_o\left[1 - e^{\left(\frac{P_R}{P_F}\right) - 1 \cdot \left(\sqrt{P_\mu}/P_R\right)}\right] e^{\left(-\sqrt{P_\mu}/P_F\right)}}{1 - \frac{P_R}{P_F}},$$

whereupon I' is $(\delta I(H)/\delta H)_{max}$ for each value of $\sqrt{P_\mu}$, I'_o is the maximum in I' without inhomogeneous broadening while P_R and P_F are exponential constants in units of $\sqrt{mW}$, respectively.

pulse sequence (Kevan and Schwartz, 1979) on moderately (top set; 30% [wt/wt] ^2H_2O) and fully hydrated (bottom set; ≥ 50% [wt/wt] ^2H_2O) nitroxyl amides. Simulations of the ESE modulation envelopes indicate that up to 4–8 ^2H_2Os bind equivalently to each nitroxyl moiety at approximately 3.6 Å with an $A_{isotropic}$ approaching 0 MHz. The computer simulation of these ESE envelopes was not facile because there could have been spectral distortion of the initial part of the time domain array caused by a small inner

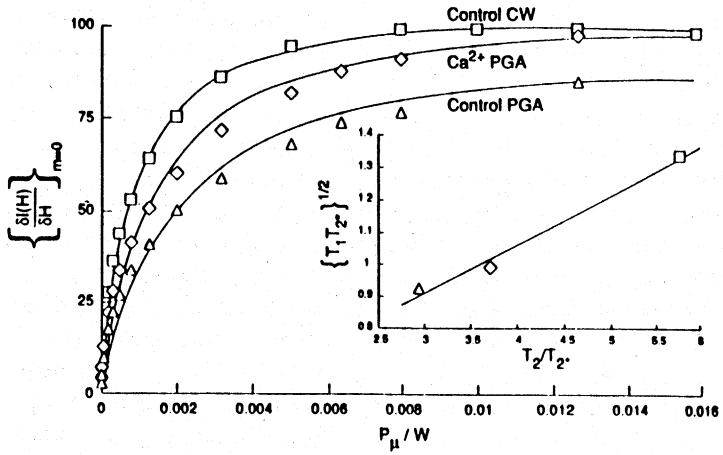

FIGURE 11-12. Partial power saturation curve (Metz et al., 1990) fit for Ca^{2+} PGA, control PGA as well as apple CW $4AT$ nitroxyl amides as a function of P_μ (in units of W). The curve fit equation used was the form,

$$I' = \frac{P_\mu^{1/2}\Psi}{(1 + \Gamma P_\mu)^{1/2}} \frac{1}{(1 + \Lambda(1 + \Gamma P_\mu)^{1/2})^2}$$

where

$$\Psi = \frac{I'_o H_1}{\sqrt{P_\mu}}, \Gamma = \frac{\gamma^2 H_1^2 T_1 T_2}{P_\mu} \text{ and } \Lambda = \frac{T_{2^*}}{T_2};$$

in our calculation we assume $H_1^2 \sim P_\mu$. Making this assumption, we find that, for the CW sample, the relaxation parameter, $\sqrt{T_1 T_2}$, was 3.21 ± 0.07 μs; the $\sqrt{T_1 T_2}$ s for the PGA matrices were 1.91 ± 0.15 and 1.58 ± 0.18 μs for the Ca^{2+} and control treatments, respectively. Inset figure: plot of the relationship between T_1 and T_2, assuming T_{2^*} is constant throughout and that $T_{2^*} \ll T_2$.

layer of bound ^2H_2O with a nominal r and nonzero $A_{isotropic}$. This potential problem is made more clear upon Fourier transformation of the time domain data (Fig. 11-14 insert, Irwin et al., 1991) whereupon a small additional peak (↑) was noted. In order to analyze the hydration process from the standpoint of the polymer (Irwin et al., 1991) a Carr-Purcell-Meiboom-Gill (Farrar, 1987) ^1H (60 MHz) NMR experiment on a comparably (e.g., to the uppermost time domain array in Fig. 11-14) hydrated sample, the paramagnetic amide of which had been previously reduced to the N–OH form, is proffered in Figure 11-15. In this experiment, the semilog plot of normalized resonance areas, as a function of the variable delay, 2τ, clearly demonstrates two populations of spin–spin relaxation. The y intercept for the slowly

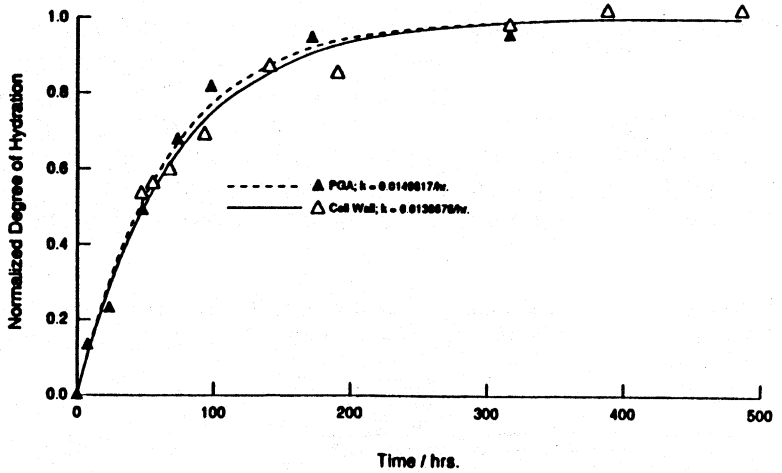

FIGURE 11-13. Dependence of polymer hydration on time in a saturated H_2O vapor chamber at 293 K. Data were fit to an exponential equation; the rate constants, k, are provided in the figure for both CW and PGA.

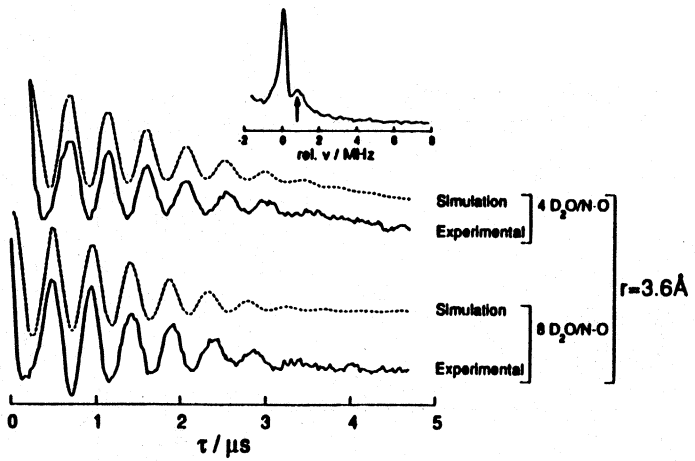

FIGURE 11-14. Three pulse electron spin-echo modulations of moderately (top) and fully hydrated (bottom) PGA nitroxyl amides at 4.2 K. The time between the first two pulses was 0.28 μs (from Chamulitrat and Irwin, 1989, with permission). Inset figure: Fourier transformation of the top experimental data.

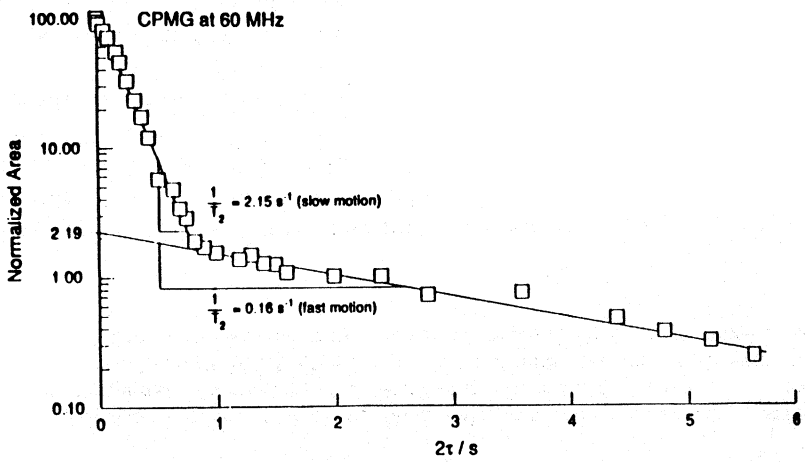

FIGURE 11-15. Carr-Purcell-Meiboom-Gill (CPMG; Farrar, 1987) refocusing spin echo ^1H (60 MHz) NMR T_2 experiment on moderately hydrated PGA nitroxyl amides at 293 K.

relaxing H_2O population (fast motion) was utilized as a relative measure of the activity of "free" H_2O presumably located in an outer hydration shell. The free H_2O was found to be only about 2% of the total hydration ^1H_2Os. For equilibrium hydrated samples, this value increases to a level >50%, whereupon there would be on the order of 10 H_2O molecules per monomer unit (Chamulitrat and Irwin, 1989).

Figure 11-16 (Irwin et al., 1991) displays how the "order parameter," $2A_{zz}$ (Chamulitrat et al., 1988), which we have shown to be related to internal nitroxyl amide reorientation about the macromolecular y-axis or main chain, changes as a function of temperature and degree of polymer hydration in spin-labeled cell wall pectinic polysaccharides. Both moderately and fully hydrated samples (10 and 168 h, respectively) had larger values of $2A_{zz}$ than the dehydrated control, possibly because of matrix deformation induced by the freezing of bound H_2O. However, there is an effect of solvent on A_{zz} that could explain these results. Notwithstanding, the temperature at which the fully hydrated sample's $2A_{zz}$ approached the 0-h observation, ca. 256 K, was remarkably similar to the temperature (T_{max}, Irwin, Sevilla, and Stoudt, 1985b) where maximal Mn^{2+} spin–spin broadening, caused by relatively close near neighbors, was observed (Fig. 11-17) for similarly hydrated CW samples. In Figure 11-17, we see that T_{max} was not associated with freezing because it was inversely related to the level of bound H_2O; however, we did find that T_{max} was related to the anionic ligand's structure. Like the T_{max} parameter, $2A_{zz}$, in the 10-h treatment, approached the dehydrated sample's

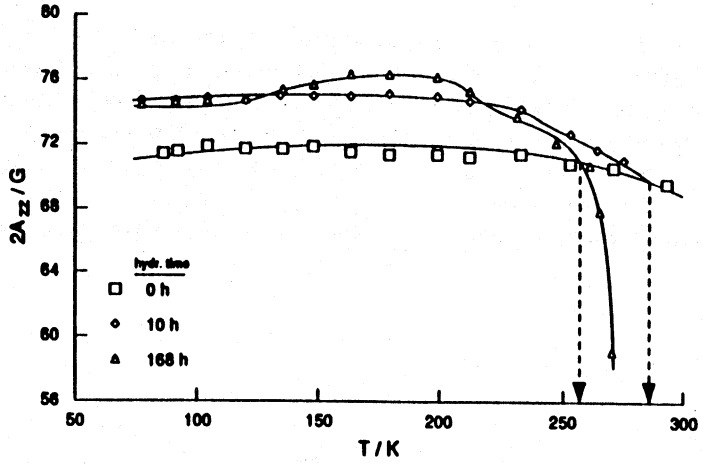

FIGURE 11-16. Dependence of the EPR nitroxyl amide parameter, $2A_{zz}$, on temperature for dehydrated (0 h), moderately hydrated (10 h) and fully hydrated (168 h) CW.

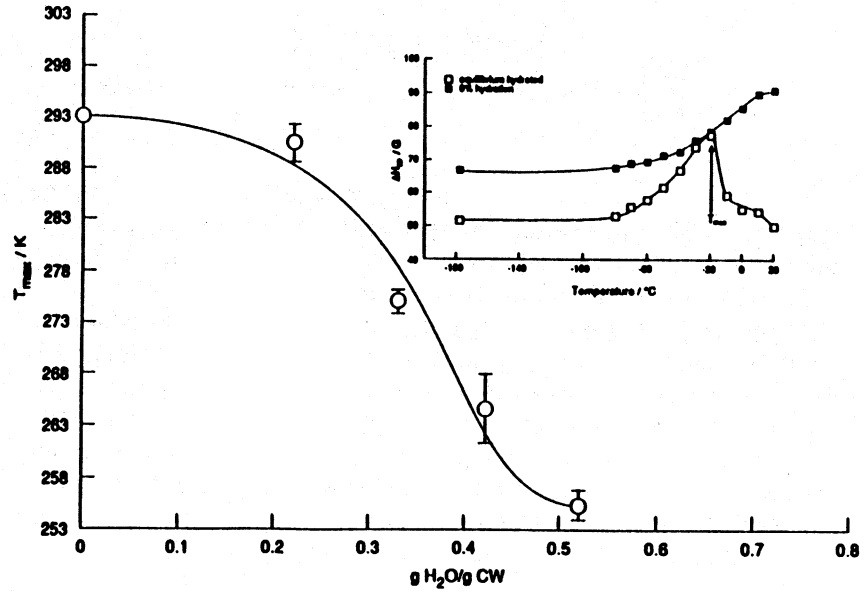

FIGURE 11-17. Dependency of T_{max} (temperature, in units of K, where maximum Mn^{2+}-filled CW linewidths were observed) on CW lattice hydration. Each data point is the mean of four replications (from Irwin et al., 1985b, with permission). Mn^{2+} levels varied between 1×10^{-4} and 3×10^{-4} mol/g (32–95% of the available sites filled). Bars represent two standard errors of each mean. Inset figure: temperature dependence of cell wall bound Mn^{2+} (6% of the available sites filled) linewidths (ΔH_{pp}) in apple CWs.

$2A_{zz}$ at or above the freezing point of bound water. If this approach to the control (0 h) $2A_{zz}$ values were due to the thawing of previously frozen bound H_2O, it would occur at a temperature much lower than what was observed, 284 K, because of the colligative property of freezing point depression (Daniels and Alberty, 1975).

Alkali extraction is the classical chemical method for removing hemicellulose, which is presumably hydrogen bonded to cellulose, from the cell wall (Fry, 1986). Unfortunately, such treatment can also break other types of bonds such as glycosidic linkages (via β- or trans-elimination; Barrett and Northcote, 1965), can hydrolyze methyl esters and acetylated groups as well as modify ionic bonds such as Ca^{2+} bridges. The CP-MAS/NMR spectrum of a 2 N KOH extracted cell wall matrix (Chamulitrat and Irwin, 1989) displayed the loss of the methyl ester's 54 ppm resonance, indicating that these were saponified concomitant with the extraction of β-*D*-glucans in hemicellulose. These alkali treatments were performed at room temperature whereupon the β-elimination process is less efficient (Barrett and Northcote, 1965); therefore, we assumed that the most significant effect of the alkali extraction was the removal of hemicellulose as well as the saponification of the methyl ester functional groups. Our EDC-mediated spin-labeling reaction was performed after the alkali treatment and EPR spectra were acquired at 77 K, as discussed in the previous section. The alkali-treated cell wall EPR spectra exhibited a *z*-axis hyperfine coupling, A_{zz}, of 36.79 G, which was significantly larger than the A_{zz} for cell walls without the alkali treatment (36.36 G for either PME-treated or control CWs). Upon fully hydrating any nitroxyl amide labeled matrix polyuronide, the EPR spectra appear as two overlapping weakly (*W*) and strongly (*S*) rotationally immobilized components (Chamulitrat and Irwin, 1989). When the nitroxyl amide labeled/alkali-treated cell wall sample was hydrated to 85% [wt/wt] and the EPR spectrum measured (Fig. 11-18, bottom; $W/S = 5.03$) the W/S ratio was much larger than the enzymatically deesterified (PME-treated, $W/S = 3.61$) cell wall matrix with a comparable level of hydration. The larger value of W/S in the hemicellulose-removed/demethylated wall matrix, relative to that of the specifically deesterified cell walls, indicates that there was an increase in the rotational freedom of the nitroxyl labels by the partial removal of hemicellulose alone. These results suggest that portions of the hemicellulose matrix must be spatially close to the labeled homopolygalacturonan chains. Upon treating the hemicellulose-removed cell walls with Ca^{+2} (0.88 cations per binding site; Fig. 11-18, top), the W/S ratio was observed to decrease from 5.0 (Fig. 11-18, bottom) to 3.6. Because the W/S parameter is a reasonable measure of the spin label's rotational freedom, this change in the population of weakly immobilized components, as a function of bound Ca^{2+}, indicates that Ca^{2+} has a strong effect on the mobility of the

spin probe and its subtending polymer. These findings are important because virtually all research into the effects of Ca^{2+} on living fruit tissue is complicated by the fact that Ca^{2+} itself has various, but not well understood, physiological effects.

As shown previously (Chamulitrat and Irwin, 1989), the behavior of hydrated CW macromolecules can be more extensively investigated when examined with respect to the diffusion of water bound to the CW polymer matrix. Upon increasing the level of hydration, the $2A_{zz}$ was attenuated, and the weakly immobilized nitroxyl amide population increased because the W/S ratio enlarged as a function of bound water. Previously (Chamulitrat et al., 1988) we recognized that there was a collapse of the apparent free volume of the polymer matrix during equilibrium hydration (e.g., as v_1 approaches v_{max}; the volume fraction of the diluent, v_1, ~ degree of hydration in units of g H_2O/g polymer). Because the translational diffusion of the penetrant, or diluent, molecules in certain polymers (Ferry, 1980) is related to free-volume theory, it is ostensibly reasonable to consider the nitroxyl amide τ_R's dependence on the H_2O of hydration in a similar manner. To this end we have modified the Fujita–Doolittle equation (Brown and Sandreczki, 1985; Chamulitrat et al., 1988; Ferry, 1980), as

$$\Xi = -\frac{1}{\log_e\left[\frac{\tau_R}{\tau_R^{ref}}\right]} = -\frac{1}{\log_e\left[\frac{(W/S)_{ref}}{(W/S)}\right]} = f_2 + \left\{\frac{f_2^2}{v_1\zeta}\right\}$$

whereupon

$$\lim_{v_1 \to v_{max}} \Xi = f_2$$

and

$$\zeta = \frac{[f_1 - f_2]}{[v_1 - v_1^{ref}]}$$

The terms f_2 and ζ are constants for a given polymer–diluent system corresponding to the free-volume fraction in the reference state (f_2) and the proportionality constant (ζ) for the dependence of the total fractional free volume, f_1, on the diluent volume fraction (v_1^{ref} is the diluent volume fraction in the dehydrated state and is assumed to be zero). We have introduced the W/S ratio (measured at room temperature) to the previous equation because we know that, for a decrease in correlation time (faster motion), there is a

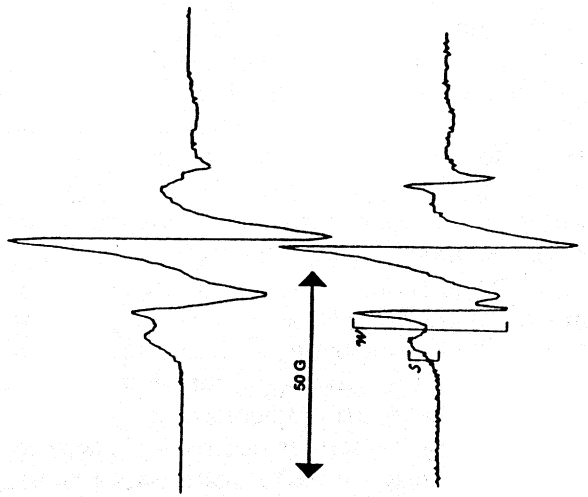

FIGURE 11-18. EPR Spectra of fully hydrated spin-labeled CW polyuronides (from Chamulitrat and Irwin, 1989, with permission). Bottom spectrum: alkali-extracted apple CW spin labeled with $4AT$. Top spectrum: Ca^{2+}-doped version of the bottom spectrum.

corresponding increase of the weakly immobilized population or W/S ratio. ζ can be obtained once the intercept and slope of a plot of $-1/\log_e[(W/S)_{ref}/(W/S)]$ versus the reciprocal of v_1 is known (Fig. 11-19). The linearity of the plots in Figure 11-19 indicate that the W/S ratios, relative to the reference or dehydrated state, are good measures of the rotational diffusion of the nitroxyl amide labels that, in turn, correlate (Chamulitrat et al., 1988) with the monomeric translational diffusion coefficient of the diluent bound to the polymer.

The experiments depicted in Figure 11-19 are evidence that ζ is a measure of "intermolecular coupling" of the labeled matrix with its surroundings (Chamulitrat and Irwin, 1989). ζs for the specifically demethylated CW homopolygalacturonans were about 58% lower than those for untreated CW. Interestingly, the PME-treated matrix had a twofold larger intermolecular coupling constant (ζ) than that of the 11% Ca^{2+} salt of PGA; this is not surprising because homopolygalacturonan blocks in the wall network are larger (Irwin, Sevilla, and Chamulitrat, 1988) than PGA, more complex, and, therefore, should have a greater degree of intermolecular coupling with near neighbor matrix polysaccharides. PGA nitroxyl amide EPR spectra were obtained at room temperature with various levels of hydration as a function of Ca^{+2}_{bound} whereupon ζs increased with increasing the percentage of Ca^{2+} bound and saturated ($\zeta_{max} \cong 4$) at approximately 0.5 bound Ca ions per site. In these studies we have assumed that the intermolecular coupling

parameter would display typical saturation behavior with respect to the fraction (Φ) of binding sites filled with Ca^{2+}. To test this idea, we have modified the Hill equation (Van Holde, 1971)

$$\zeta = \frac{\zeta_{obs}}{\zeta_{max}} = \frac{K\Phi^n}{1 + K\Phi^n}$$

$$\frac{\zeta}{1-\zeta} = K\Phi^n$$

$$\log_{10}\left\{\frac{\zeta}{1-\zeta}\right\} = \log_{10}K + n\log_{10}\Phi,$$

whereupon ζ_{max} was estimated to be approximately 4, K is an arbitrary constant, and n, the Hill coefficient, is a measure of a system's cooperativity at equilibrium. The previous linearized log–log equation is shown in Figure 11-19 (insert; $n = 2.98 \pm 0.15$). In normal, solution phase, usage ζ would be

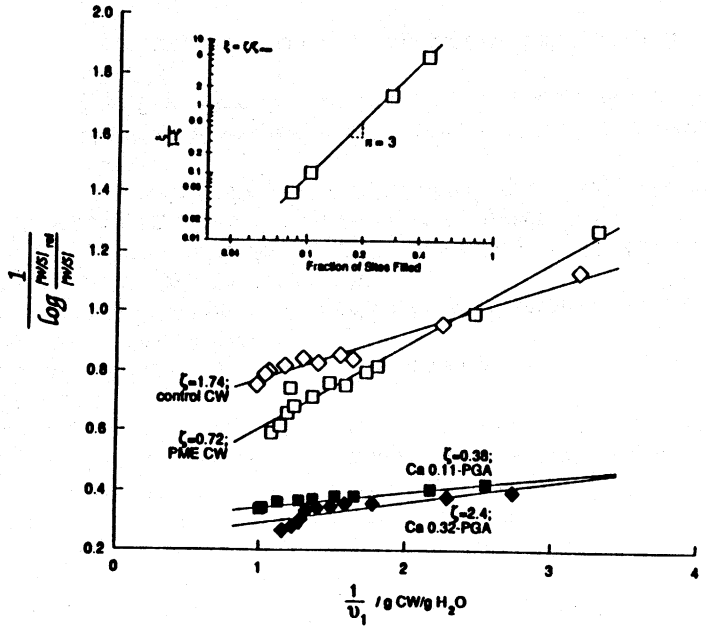

FIGURE 11-19. Fugita–Doolittle plots of variously treated 4*AT* spin-labeled PGA and CWs (from Chamulitrat and Irwin, 1989, with permission). Insert figure: Hill plot showing the dependence of PGA nitroxyl amide ζ, derived from Fugita–Doolittle plots, on the fraction of binding sites filled with Ca^{2+}. The slope gives $n = 3$, which is evidence for highly positive cooperative Ca^{2+} binding (see text).

treated as the fractional saturation of an ensemble of binding sites ($\bar{\alpha}$) on a macromolecule, Φ as the total initial concentration of the ligand (A_L), and K as an equilibrium constant. However, if ζ is a parameter sensitive to the spatial organization of the Ca^{2+} cross-linkages in the polyuronic acid matrix, then its behavior with respect to Φ, the faction of sites filled with Ca^{2+}, should be similar to $\bar{\alpha}$ as a function of A_L in a cooperative Ca^{2+} binding system such as the homopolygalacturonans (Irwin, Sevilla, and Shieh, 1984; Irwin, Sevilla, and Stoudt, 1985b). Such behavior argues that ζ is a parameter that describes the spatial distribution of the Ca^{2+} cross-linkages; thus, if $n \sim 1$, the distribution is random, whereas if n is much larger than 1, the cations are distributed in a spatially nonrandom or sequential fashion as has been proposed before (Irwin, Sevilla, and Stoudt, 1985b; Irwin, Sevilla, and Shieh, 1984) for paramagnetic divalent cations.

SUMMARY

All the experiments that we have presented herein as examples of the spin label technique indicate that these methods can be applied to food systems for the purpose of characterizing perturbations induced by weak intermolecular forces, such as Ca^{2+} bridges, on hydration-deformed or dehydrated sugar acid polysaccharides. We have shown the mechanism of covalent attachment of the spin label, 4*AT*, to acid polysaccharides; we have utilized various types of spectral simulations to calculate τ_R; we have used the temperature dependence of τ_R to determine divergent E_as for different types of molecular motion (local and internal motions); and, last, we have delved into the perturbations in the higher-order structure and mobility of the sugar acid-containing matrix polysaccharide chains induced by ionic cross-bonding as well as other weak forces upon equilibrium hydration.

References

Abragam, A., and B. Bleaney. 1970. *Electron Paramagnetic Resonance of Transition Ions.* Oxford: Oxford University Press.

Barrett, A., and D. Northcote. 1965. Apple Fruit Pectic Substances. *Biochem. J.* **94**:617–627.

Ben-Arie, R., N. Kisley, and C. Frenkel. 1979. Ultrastructural changes in the cell walls of ripening apple and pear fruit. *Plant Physiol.* **64**:197–202.

Berliner, L. 1976. *Spin Labeling: Theory and Applications,* Vols. 1 & 2. New York: Academic Press.

Bloembergen, N., E. Purcell, and R. Pound. 1945. Relaxation effects in nuclear magnetic resonance absorption. *Phys. Rev.* **73**:679–712.

Brown, I., and T. Sandreczki. 1985. Motional correlation times of nitroxide spin labels and spin probes in an amine-cured epoxy resin: solvent dependence. *Macromolecules* **18**:2702–2709.

Cesaro, A., A. Ciana, T. Delben, G. Manzini, and S. Paoletti. 1982. Physicochemical Properties of Pectic Acid. I. Thermodynamic Evidence of a pH-Induced Conformational Transition in Aqueous Solution. *Biopolymers* 21:431–449.

Chamulitrat, W., and P. Irwin. 1989. Homopolygalacturonan Nitroxyl Amides: Matrix Deformation Induced Motional Perturbations of Cell Wall Polyuronides. *Macromolecules* 22:2685–2693.

Chamulitrat, W., P. Irwin, L. Sivieri, and R. Schwartz. 1988. Homopolygalacturonan Nitroxyl Amides: Hydration-induced Motion. *Macromolecules* 21:141–146.

Daniels, F., and R. Alberty. 1975. *Physical Chemistry,* 4th ed. New York: John Wiley & Sons.

Darvill, A., M. McNeil, P. Albersheim, and D. Delmer. 1980. *The Biochemistry of Plants,* Vol. I, 91–162. New York: Academic Press.

Dea, I., E. Morris, D. Rees, J. Welsh, H. Barnes, and J. Price. 1977. Associations of like and unlike polysaccharides: mechanism and specificity in galactomannans, interacting bacterial polysaccharides, and related systems. *Carbohydr. Res.* 57:249–272.

Eaton, S., and G. Eaton. 1978. Interaction of Spin Labels with Transition Metals. *Coord. Chem. Rev.* 26:207–262.

Eaton, D., and W. Phillips. 1965. Nuclear magnetic resonance of paramagnetic molecules. *Adv. Mag. Res.* 1:103–148.

Farrar, T. 1987. *Pulse Nuclear Magnetic Resonance Spectroscopy, An Introduction to the Theory and Applications,* 55–57. Chicago: Farragut Press.

Ferry, J. 1980. *Viscoelastic Properties of Polymers,* 3rd ed., 486–496. New York: John Wiley & Sons.

Fishman, M., P. Pfeffer, R. Barford, and L. Doner. 1984. Studies of pectin solution properties by high performance size exclusion chromatography. *J. Agric. Food Chem.* 32:372–378.

Freed, J. 1976. *Spin Labelling: Theory and Applications,* Vol. 1, 53–132. New York: Academic Press.

Fry, S. 1986. Cross-linking of matrix polymers in the growing cell walls of angiosperms. *Annu. Rev. Plant Physiol.* 37:165–186.

Gerasimowicz, W., K. Hicks, and P. Pfeffer. 1984. Evidence for the existence of associated lignin-carbohydrate polymers as revealed by carbon-13 CP-MAS solid-state NMR spectroscopy. *Macromolecules* 17:2597–2603.

Gnewuch, T., and G. Sosnovsky. 1986. Spin-labeled Carbohydrates. *Chem. Rev.* 86:203–238.

Grant, G., E. Morris, D. Rees, P. Smith, and D. Thom. 1973. Biological interactions between polysaccharides and divalent cations: The egg-box model. *FEBS Lett.* 32:195–198.

Hoare, D., and D. Koshland, Jr. 1967. A method for the quantitative modification and estimation of carboxylic acid groups in proteins. *J. Biol. Chem.* 242:2447–2453.

Hyde, J., and K. Rao. 1978. Dipolar-induced electron spin-lattice relaxation in unordered solids. *J. Magn. Reson.* 29:509–516.

Irwin, P., W. Chamulitrat, M. Sevilla, and A. Hoffman. 1991. Unpublished Data.

Irwin, P., W. Gerasimowicz, P. Pfeffer, and M. Fishman. 1985a. ^{1}H-^{13}C polarization transfer studies of uronic acid polymer systems. *J. Agric. Food Chem.* 33:1197–1201.

Irwin, P., M. Sevilla, and W. Chamulitrat. 1988. Homopolygalacturonan molecular size in plant cell wall matrices via paramagnetic ion and nitroxyl amide dipolar spin-spin interactions. *Biophys. J.* 54:337–344.

Irwin, P., M. Sevilla, and S. Osman. 1987. Spectroscopic Evidence for Spatially Sequential Amide Bond Formation in Plant Homopolygalacturonans. *Macromolecules* 20:1222–1227.

Irwin, P., M. Sevilla, and J. Shieh. 1984. ESR Evidence of Sequential Divalent Cation Binding in Higher Plant Cell Walls. *Biochim. Biophys. Acta* 805:186–190.

Irwin, P., M. Sevilla, and C. Stoudt. 1985b. EPR spectroscopic evidence for hydration- and temperature-dependent spatial perturbations of a higher plant cell wall paramagnetic ion lattice. *Biochim. Biophys. Acta* 842:76–83.

Jarvis, M. 1984. Structure and properties of pectin gels in plant cell walls. *Plant Cell Environ.* 7:153–164.

Kevan, L., and R. Schwartz. 1979. *Time Domain Electron Spin Resonance,* 279–341. New York: John Wiley & Sons.

Leigh, J. S., Jr. 1970. ESR rigid-lattice line shape in a system of two interacting spins. *J. Chem. Phys.* 52:2608–2612.

McMillan, J. 1968. *Electron Paramagnetism,* 153–173. New York: W. A. Benjamin, Inc.

Metz, H., G. Völkel, and W. Windsch. 1990. A Simple Method for Fitting of Inhomogeneous ESR Saturation Curves. *Phys. Stat. Sol. A (App. Res.)* 122:K73–K76.

Poole, C., Jr. 1983. *Electron Spin Resonance, A Comprehensive Treatise on Experimental Techniques.* New York: John Wiley & Sons.

Preston, R. 1979. The physical biology of plant cell walls. *Annu. Rev. Plant Physiol.* 30:55–78.

Pryce, M., and K. Stevens. 1950. The theory of magnetic resonance-line widths in crystals. *Proc. Phys. Soc. (Lond.)* A63:36–51.

Redfield, A. 1965. The theory of relaxation processes. *Adv. Mag. Res.* 1:1–32.

Rees, D., E. Morris, D. Thom, and J. Madden. 1982. *The Polysaccharides,* 195–290. New York: Academic Press.

Stevens, B., and R. Selvendran. 1984. Structural features of cell-wall polymers of the apple. *Carbohydr. Res.* 135:155–166.

Swartz, H., J. Bolton, and D. Borg. 1972. *Biological Applications of Electron Spin Resonance.* New York: John Wiley & Sons.

Taylor, R., and H. Conrad. 1972. Stoichiometric depolymerization of polyuronides and glycosaminoglycuronans to monosaccharides following reduction of their carbodiimide-activated carboxyl groups. *Biochemistry* 11:1383–1388.

Van Holde, K. 1971. *Physical Biochemistry,* 57–65. Englewood Cliffs, NJ: Prentice-Hall.

Van Vleck, J. H. 1948. The dipolar broadening of magnetic resonance lines in crystals. *Phys. Rev.* 74:1168–1183.

Wertz, J., and J. Bolton. 1986. *Electron Spin Resonance, Elementary Theory and Practical Applications.* New York: Chapman and Hall.